Multi-Beam Multiplexing Design with Phase-Only Excitation Based on Hybrid Beamforming Architectures

Junwei Zhang*†, Shufeng Li*†, Libiao Jin*†, Wei Liu* and Hing Cheung So†

*†School of Information and Communication Engineering, Communication University of China, Beijing, China

*School of Electronic Engineering and Computer Science, Queen Marry University of London, London, UK

†Department of Electrical Engineering, City University of Hong Kong, Hong Kong, China

Introduction

Since the weighting coefficient associated with each antenna is a complex number, both magnitude and phase controls are required in analog implementation and they are different for different antennas. This will add complexity to its implementation especially for large-scale antenna arrays and this problem can be mitigated by phase-only control on the analog beamformer.

Here a novel design is proposed based on the work in [1], where a phase-only control is considered so that the magnitude of weighting coefficients can be precomputed by the designers in advance according to their specified requirements.

Review of sub-connected hybrid beamformer

A hybrid beamforming structure based on an F-antenna uniform linear array (ULA) configured with the interleaved and localised subarray architectures is shown in Figs. 1 and 2, respectively, where the inter-element spacing is d. The whole array is grouped into N subarrays and each subarray has $Z = \frac{F}{N}$ antennas with an adjacent spacing $d_n = Nd$ and $d_n = d$ for the interleaved and localised subarray architectures, respectively.

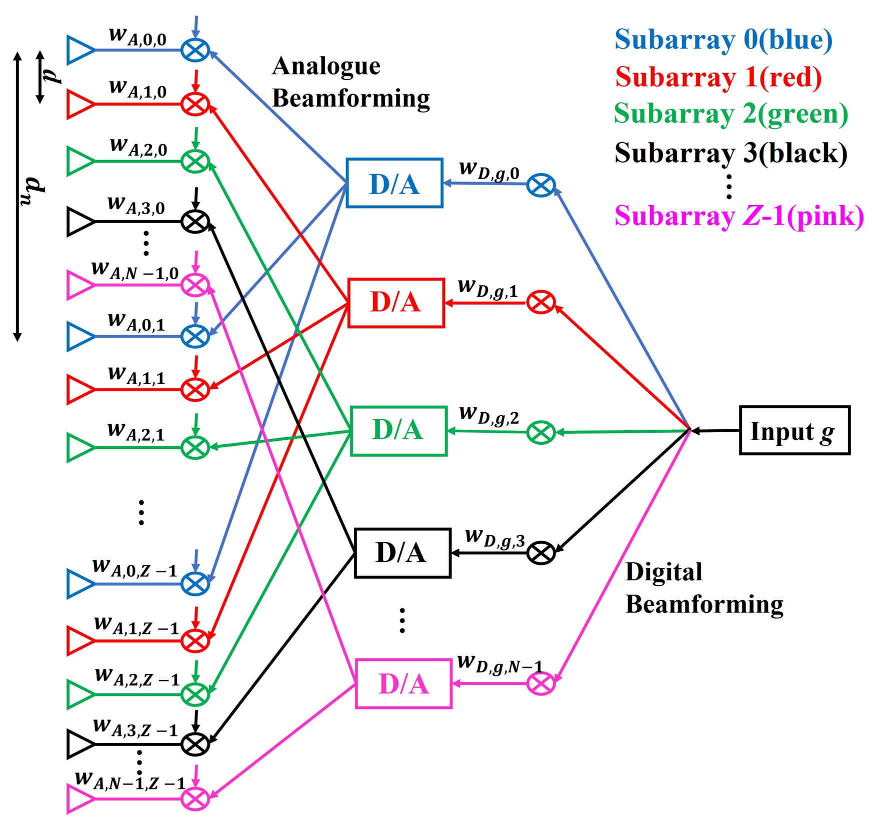

Figure 1: Interleaved subarray architecture.

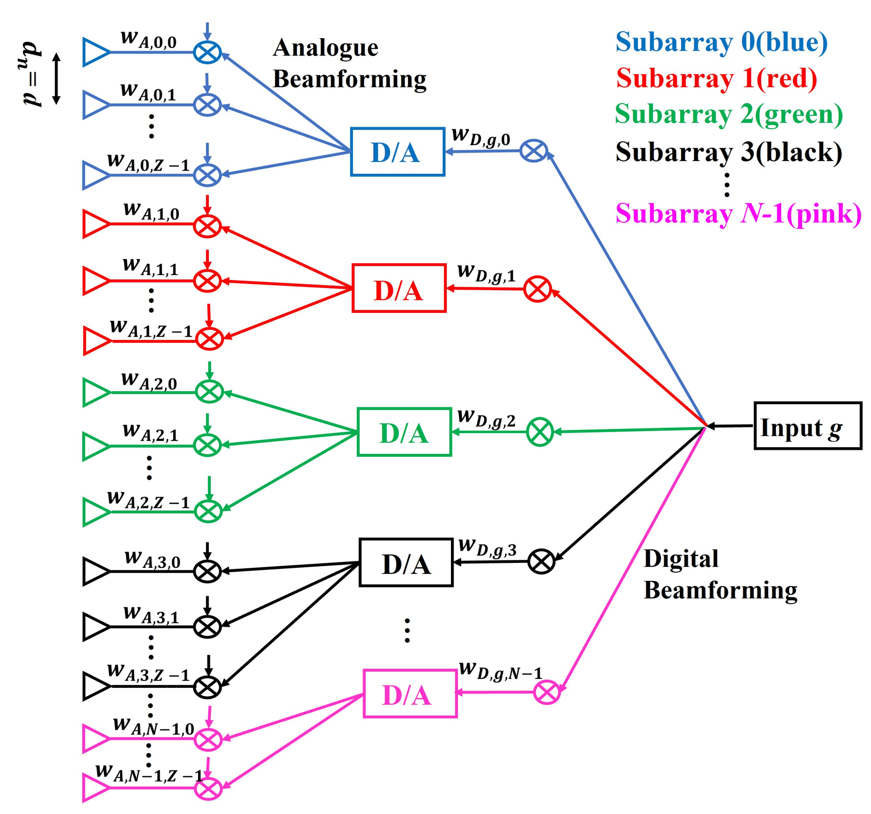

Figure 2: Localised subarray architecture.

The steering vector of the n-th subarray with the interleaved and localised subarray architectures is respectively expressed as

$$\boldsymbol{v}_n(\theta) = [e^{j2\pi n\frac{d}{\lambda}\sin\theta}, e^{j2\pi(n+N)\frac{d}{\lambda}\sin\theta}, ..., e^{j2\pi(n+N(Z-1))\frac{d}{\lambda}\sin\theta}]^T, \tag{1}$$

$$\boldsymbol{v}_n(\theta) = [e^{j2\pi nZ\frac{d}{\lambda}\sin\theta}, e^{j2\pi(nZ+1)\frac{d}{\lambda}\sin\theta}, ..., e^{j2\pi((n+1)Z-1)\frac{d}{\lambda}\sin\theta}]^T, \tag{2}$$

where $[\cdot]^T$ is the transpose operator, λ the signal wavelength.

The analog response generated by the n-th subarray is $R_{A,n}(\theta) = \boldsymbol{w}_{A,n}^H\boldsymbol{v}_n(\theta)$, where $[\cdot]^H$ represents the Hermitian transpose and $\boldsymbol{w}_{A,n}$ is the corresponding analog coefficient vector $\boldsymbol{w}_{A,n} = [w_{A,n,0}, w_{A,n,1}, ..., w_{A,n,Z-1}]^T$, is the corresponding analog coefficient vector. Through grouping the analog beam response of N subarrays for the g-th beam into one vector

$$\boldsymbol{r}_{A,g}(\theta) = [R_{A,0}(\theta), R_{A,1}(\theta), ..., R_{A,N-1}(\theta)]^T, \tag{3}$$

where $g \in \{0, 1, ..., G-1\}$, the designed beam response is formulated as $R_{\varphi_g}(\theta) = \boldsymbol{w}_{D,g}^H\boldsymbol{r}_{A,g}(\theta)$, where $\boldsymbol{w}_{D,g}$ represents the digital coefficient vector for the g-th beam, given by $\boldsymbol{w}_{D,g} = [w_{D,g,0}, w_{D,g,1}, ..., w_{D,g,N-1}]^T$.

The digital pattern created by the z-th antenna of the n-th subarray for the g-th beam is written as $R_{D,g,n,z}(\theta) = \boldsymbol{w}_{D,g}^H\check{\boldsymbol{v}}_z(\theta)$, with $\check{\boldsymbol{v}}_z(\theta) = [v_{0,z}(\theta), v_{1,z}(\theta), ..., v_{N-1,z}(\theta)]^T$. By combining the digital response of Z antennas in the n-th subarray into one vector, given by

$$\boldsymbol{r}_{D,g,n}(\theta) = [R_{D,g,n,0}(\theta), R_{D,g,n,1}(\theta), ..., R_{D,g,n,Z-1}(\theta)]^T, \tag{4}$$

the g-th beam response can also be expressed as $R_{\varphi_g}(\theta) = \boldsymbol{w}_{A,n}^H\boldsymbol{r}_{D,g,n}(\theta)$.

Constant magnitude constraint on analog coefficients

The sum of sidelobe responses for G beams can be approximately formulated as $K_{sl} = \sum_{g=0}^{G-1}\sum_{\theta\in\Theta_{side_g}}\left|R_{\varphi_g}(\theta)\right|^2$, where Θ_{side_g} represents the sidelobe region of the g-th beam. With $R_{\varphi_g}(\theta) = \boldsymbol{w}_{A,n}^H\boldsymbol{r}_{D,g,n}(\theta)$, K_{sl} is changed to $K_{sl_{\boldsymbol{w}_A}} = \sum_{g=0}^{G-1}\sum_{n=0}^{N-1}\sum_{\theta\in\Theta_{side_g}}\boldsymbol{w}_{A,n}^H\boldsymbol{r}_{D,g,n}(\theta)\boldsymbol{r}_{D,g,n}^H(\theta)\boldsymbol{w}_{A,n}$, where $\boldsymbol{w}_{A,n}$ for $n \in \{0, 1, ..., N-1\}$ can be combined into a new vector $\boldsymbol{w}_A = [\boldsymbol{w}_{A,0}^T, \boldsymbol{w}_{A,1}^T, ..., \boldsymbol{w}_{A,N-1}^T]^T$. Subject to the mainlobe of each of the designed beams pointing to the desired direction, the total sidelobe response is minimised with the following formulation

$$\min_{\boldsymbol{w}_A} \quad K_{sl_{\boldsymbol{w}_A}} \text{s.j.} \quad \boldsymbol{w}_A^H\begin{bmatrix} \tilde{\boldsymbol{w}}_{D,0,0}^H\boldsymbol{c}_{0,0} & \cdots & \tilde{\boldsymbol{w}}_{D,G-1,0}^H\boldsymbol{c}_{G-1,0} \\ \tilde{\boldsymbol{w}}_{D,0,1}^H\boldsymbol{c}_{0,1} & \cdots & \tilde{\boldsymbol{w}}_{D,G-1,1}^H\boldsymbol{c}_{G-1,1} \\ \vdots & \ddots & \vdots \\ \tilde{\boldsymbol{w}}_{D,0,N-1}^H\boldsymbol{c}_{0,N-1} & \cdots & \tilde{\boldsymbol{w}}_{D,G-1,N-1}^H\boldsymbol{c}_{G-1,N-1} \end{bmatrix} = \boldsymbol{q}, \tag{5}$$

with

$$\tilde{\boldsymbol{w}}_{D,g,n} = w_{D,g,n}\boldsymbol{I}_Z, \quad \boldsymbol{c}_{g,n} = \sum_{\theta\in\Theta_{main_g}}\boldsymbol{v}_n(\theta), \tag{6}$$

where $\boldsymbol{I}_Z$ and $\boldsymbol{q}$ are the $Z \times Z$ identity matrix and $1 \times G$ all-one vector, respectively, and Θ_{main_g} denotes the mainlobe direction of the g-th beam.

However, the magnitudes of the analog coefficients obtained by (5) are distinct, and an individual feed circuit for each antenna is required for analog beamforming. For phase-only control, a new constraint is given by $|\boldsymbol{w}_A| = \boldsymbol{x} = [\chi_0, \chi_1, ..., \chi_{F-1}]^T$, where $|\cdot|$ is the element-wise absolute value operator.

The new formulation to optimise the weighting coefficients is given by

$$\min_{\boldsymbol{w}_A,\boldsymbol{\psi}} \quad K_{sl_{\boldsymbol{w}_A}} \text{subject to the constraint in (5),} \quad \Re\left\{\boldsymbol{w}_A \circ e^{-j\boldsymbol{\psi}}\right\} = \boldsymbol{x}. \tag{7}$$

Next, when $\boldsymbol{w}_A$ is known, the optimum digital coefficient vector can be calculated as follows.

By substituting $R_{\varphi_g}(\theta) = \boldsymbol{w}_{D,g}^H\boldsymbol{r}_{A,g}(\theta)$ into K_{sl}, K_{sl} can be rewritten as

$$K_{sl_{\boldsymbol{w}_D}} = \sum_{g=0}^{G-1}\sum_{n=0}^{N-1}\sum_{\theta\in\Theta_{side_g}}\boldsymbol{w}_{D,g}^H\boldsymbol{r}_{A,g}(\theta)\boldsymbol{r}_{A,g}^H(\theta)\boldsymbol{w}_{D,g}, \tag{8}$$

where $\boldsymbol{w}_{D,g}$ for $g \in \{0, 1, ..., G-1\}$ can be combined into a vector $\boldsymbol{w}_D = [\boldsymbol{w}_{D,0}^T, \boldsymbol{w}_{D,1}^T, ..., \boldsymbol{w}_{D,G-1}^T]^T$.

Given the obtained $\boldsymbol{w}_A$ in (7), the formulation to find the digital coefficient vector $\boldsymbol{w}_D$ is given by

$$\min_{\boldsymbol{w}_D} \quad K_{sl_{\boldsymbol{w}_D}} \quad \text{s.j.} \quad \boldsymbol{B}^H\boldsymbol{w}_D = \boldsymbol{q}^T, \quad \text{with} \tag{9}$$

$$\boldsymbol{B} = \begin{bmatrix} \boldsymbol{w}_A^H\hat{\boldsymbol{t}}_{0,0} & 0 & \cdots & 0 \\ \vdots & \ddots & \ddots & \vdots \\ \boldsymbol{w}_A^H\hat{\boldsymbol{t}}_{0,N-1} & \ddots & 0 & 0 \\ \vdots & \boldsymbol{w}_A^H\hat{\boldsymbol{t}}_{1,0} & \ddots & \vdots \\ \vdots & \ddots & \ddots & \vdots \\ 0 & \cdots & \cdots & \boldsymbol{w}_A^H\hat{\boldsymbol{t}}_{G-1,N-1} \end{bmatrix}, \quad \hat{\boldsymbol{t}}_{g,0} = \begin{bmatrix} \boldsymbol{c}_{g,0} \\ \boldsymbol{0}_{Z\times1} \\ \vdots \\ \boldsymbol{0}_{Z\times1} \end{bmatrix}, \ \vdots \ \hat{\boldsymbol{t}}_{g,N-1} = \begin{bmatrix} \boldsymbol{0}_{Z\times1} \\ \boldsymbol{0}_{Z\times1} \\ \vdots \\ \boldsymbol{c}_{g,N-1} \end{bmatrix}, \tag{10}$$

where $\boldsymbol{0}_{Z\times1}$ in (10) is the $Z \times 1$ all-zero vector.

Alternating optimisation of $\boldsymbol{w}_D$, $\boldsymbol{w}_A$ and $\boldsymbol{\psi}$ is as follows:

(1) First, via initialising $\boldsymbol{w}_D$ randomly, $\boldsymbol{w}_A$ is computed by (5).

(2) Based on the optimum value for $\boldsymbol{w}_A$ computed in last step, the angle $\boldsymbol{\psi}$ is computed by $\boldsymbol{\psi} = \angle\boldsymbol{w}_A$.

(3) With the $\boldsymbol{\psi}$ in step (2), the new $\boldsymbol{w}_A$ can be computed by (7).

(4) Repeat steps (2) and (3) until convergence.

(5) Based on the optimum value for $\boldsymbol{w}_A$ computed in step (4), the optimum value for $\boldsymbol{w}_D$ is found by (9).

(6) Given the value of $\boldsymbol{w}_D$ in step (5), the new $\boldsymbol{w}_A$ can be updated by steps (2), (3) and (4).

(7) Repeat steps (2) - (6) until convergence.

Design examples

The two beam directions are $\varphi_0 = -30^\circ$ and $\varphi_1 = 20^\circ$ and the sidelobe regions are $\sin\Theta_{S_0} \in [-1, -0.55] \cup [-0.45, 1]$ and $\sin\Theta_{S_1} \in [-1, 0.29] \cup [0.39, 1]$.

Moreover, $F = 2Z = 50$ antennas are considered and the antenna spacing is $d = 0.3\lambda$. Apart from the example generated by (5), one special case is considered, i.e., $\chi_f = 1/48 \approx 0.0208$, where $f \in \{0, 1, ..., 49\}$, for the weighting coefficients with equal-magnitude constraint.

Overall results obtained by the proposed design (7) with different subarray architectures are presented in Figs. 3 and 4, respectively.

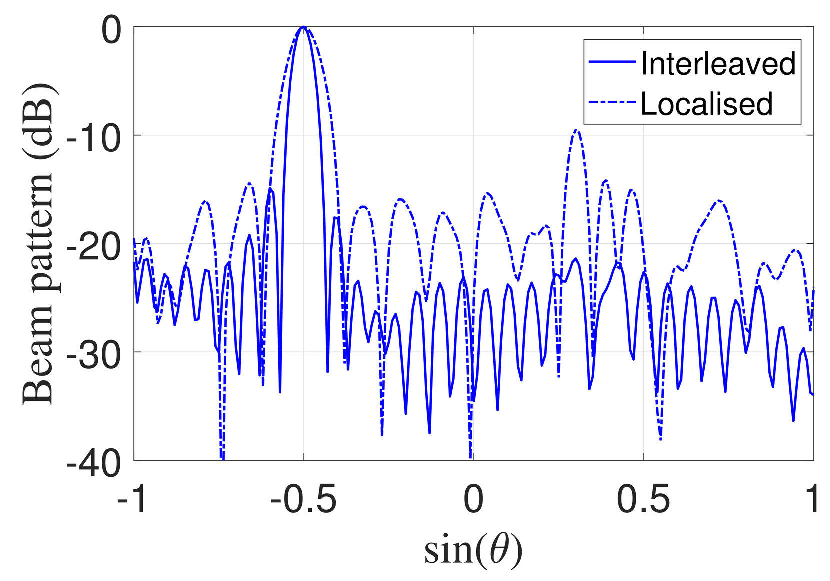

Figure 3: Resultant responses of the 0th beam generated by design (7).

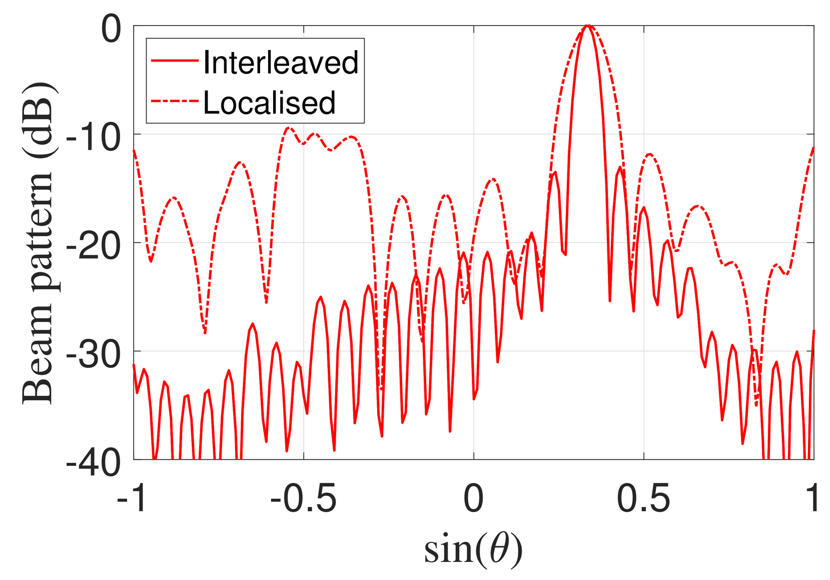

Figure 4: Resultant responses of the 1st beam generated by design (7).

The mean value for the total sidelobe responses is calculated by $\bar{R}_{side} = \frac{1}{GY_s}\sum_{g=0}^{G-1}\sum_{j=0,\theta_j\in\Theta_{side_g}}^{Y_s-1}\left|R_{\varphi_g}(\theta_j)\right|^2$ and the normalised variance for the magnitudes of $\boldsymbol{w}_A$ is defined as $\delta_{|\boldsymbol{w}_A|} = \frac{1}{F}\sum_{f=0}^{F-1}\frac{||\boldsymbol{w}_A(f)|-|\bar{\boldsymbol{w}}_A||^2}{|\bar{\boldsymbol{w}}_A|^2}$, where $|\bar{\boldsymbol{w}}_A| = \frac{1}{F}\sum_{f=0}^{F-1}|\boldsymbol{w}_A(f)|$. The comparison for different designs is summarised in Table 1.

Table 1: Summary of performance metrics for different designs.

	Structure	$\bar{R}_{side}$(dB)	$\delta_{\vert\boldsymbol{w}_A\vert}$	$t(s)$
Design (5)	Interleaved	-25.12	0.3764	8.66
	Localised	-19.79	0.9535	2.28
Design (7)	Interleaved	-22.90	1.189×10^{-11}	78.71
	Localised	-14.50	7.345×10^{-4}	44.94

For each of the two designs, although the computational time for the design based on the interleaved architecture is longer than that of the design with the localised one, it gives a narrower beamwidth for each of the designed beams with lower sidelobe responses and variance on analog weighting magnitudes.

Conclusions

A constant magnitude constraint is enforced in multi-beam multiplexing design based on a hybrid massive MIMO beamforming structure so that a phase-only control is achieved by maintaining the circuit gain at a fixed value. In addition, the analog magnitudes of the weighting coefficients for all antennas can be predetermined in advance to meet specific application requirements. Although the constraint to limit the magnitude of the analog coefficients is non-convex, it can be transformed to a convex one through an iterative phase compensation method.

References

[1] J. Zhang, W. Liu, C. Gu, S. Gao, and Q. Luo, "Robust multi-beam multiplexing design based on a hybrid beamforming structure with nearly equal magnitude analogue coefficients," *IEEE Trans. Veh. Technol.*, vol. 71, no. 5, pp. 5564–5569, May 2022.